Jason-3 GDR
Quality Assessment Report

Cycle 016

15-07-2016 / 25-07-2016

Prepared by :	H. Roinard , CLS O. Lauret , CLS S. Labroue , CLS F. Piras , CLS	
Accepted by :	DT/AQM , CLS	
Approved by :	J-D. Desjonqueres , CNES	

CLS
COLLECTE LOCALISATION SATELLITES

SALP
Service Altimetrie & Localisation Precise

SALP-RP-JALT3-EX-23103-CLS016
Edition 01.0, May 2017

1. Introduction

1.1. Document overview

The purpose of this document is to report the major features of the data quality from the Jason-3 mission. The document is associated with data dissemination on a cycle per cycle basis.
This document reports results from Jason-3 GDRs.
The objectives of this document are :

To provide a data quality assessment
To provide users with necessary information for data processing
To report any change likely to impact data quality at any level, from instrument status to software configuration
To present the major useful results for the current cycle

1.2. Software version

The results presented in this report have been performed with GDR products in version D. A detailed description of the products can be found in the Jason-3 user handbook ([1]). This cycle has been produced with the Processing Software references :
L1 library=V4.5p1, L2 library=V5.3p1p2p3p4p5p6p7p9, Processing Pilot=4.5

1.3. Cycle quality and performances

Data quality for this cycle is nominal.

Analysis of crossovers and sea surface variability indicate that system performances are close to usual values that are obtained from TOPEX/POSEIDON, Jason-1 or Jason-2 data. For this cycle, the crossover standard deviation is 5.96 cm rms. When using a selection to remove shallow waters (1000 m), areas of high ocean variability and high latitudes ($> |50|$ deg.) it decreases down to 5.16 cm rms.

The standard deviation of Sea Level Anomalies (SLA) relative to a 7-year mean (based on T/P data) is 10.54 cm. When using a selection to remove shallow waters (1000 m), areas of high ocean variability and high latitudes ($> |50|$ deg) it lowers to 8.88 cm .

— Performances from crossover differences are detailed in the dedicated **section Crossover statistics**.
— Detailed CALVAL results are presented in **section 3**.

During this cycle the following events occured :
— Yaw Ramp(Fixed to Sinusoid BETAP=-14.8) on 2016-07-20 from 00 :25 :27 to 00 :27 :03 (Pass 125)

1.4. Information about tracking mode

Jason-3 is able to track data with several onboard tracker modes : the Autonomous mode using Median algorithm (also called Median mode) and the Diode/DEM mode. Median mode is similar to the one used by Jason-2. Diode/DEM mode is a technique also used on Jason-2 using information coming from Diode and a digital elevation model available onboard. In addition to Jason-2, Jason-3 Diode/DEM mode has a new option to switch automatically between Diode/DEM mode to Median mode depending on the satellite position. For more information about the different onboard tracker algorithms see [4] (about Jason-2).
During this cycle, Jason-3 used Diode/DEM mode.

2. Data coverage and edited measurements

This section presents results that illustrate data quality during this cycle. These verification products are produced operationally so that they allow long term monitoring of missing and edited measurements.

2.1. Missing measurements

This cycle has no missing pass, but a part of pass 175 is missing on 2016-07-21 between 23 :11 :10 and 23 :12 :42 (about latitude of -62 degrees). Missing measurements relative to a nominal ground track are plotted on figure 1.

The map below illustrates missing 1Hz measurements in the GDRs, with respect to a 1 Hz sampling of a nominal repeat track. Missing measurements occur over land, especially regions with high relief. This is an expected behaviour of altimeter tracking loop. In addition, there are missing measurements over instrument calibration areas.

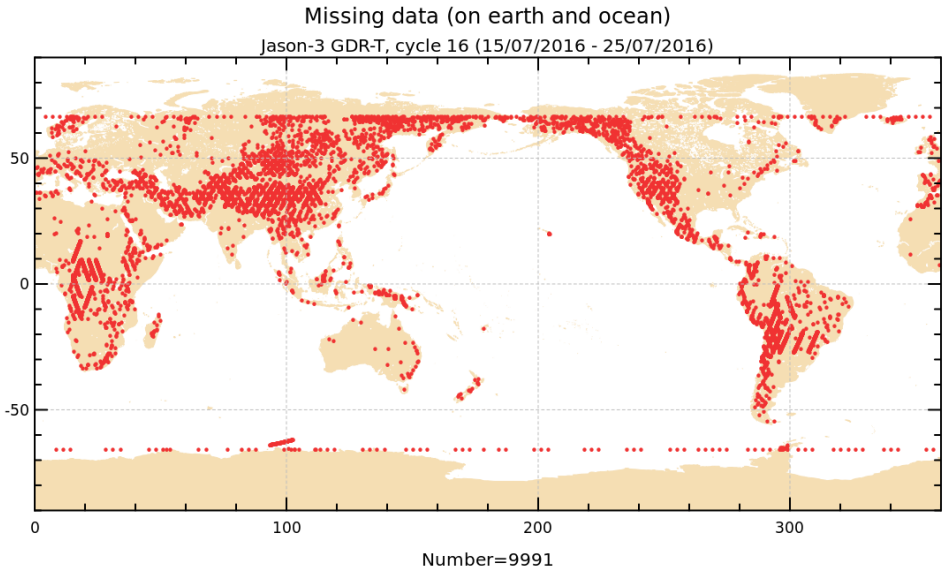

FIGURE 1 – *Missing measurements for cycle 016.*

2.2. Edited measurements

Editing criteria are defined for the GDR product in Jason-3 User Handbook [1].
The editing criteria are defined as minimum and maximum thresholds for various parameters. Measurements are edited if at least one parameter does not lie within those thresholds. These thresholds are expected to remain constant throughout the Jason-3 mission, so that monitoring the number of edited measurements allows a survey of data quality.
The rain flag is not used for data selection.

The number and percentage of points removed over ocean by each criterion is given on the following table. Note that these statistics are obtained with measurements already edited for ice flag (8.51 % of points removed).

Parameters	Min threshold	Max threshold	Unit	Nb removed	% removed
Combined atmospheric correction	-2	2	m	0	0.00
Dry tropospheric correction	-2.5	-1.9	m	0	0.00
Ionospheric correction	-0.4	0.04	m	6514	1.24
Ocean tide	-5	5	m	40	0.01
Equilibrium tide	-0.5	0.5	m	0	0.00
Pole tide	-15	15	m	0	0.00
Nb measurements of range	10	20	_	5793	1.10
Std. deviation of range	0	0.2	m	8018	1.53
Sea State Bias	-0.5	0	m	2749	0.52
Sea surface height	-130	100	m	4187	0.80
Backscatter coefficient	7	30	dB	2940	0.56
Nb measurements of sigma0	10	20	_	5734	1.09
Std. deviation of sigma0	0	1	dB	12612	2.40
Sea level anomaly	-2	2	m	4589	0.87
Earth tide	-1	1	m	0	0.00
Square off nadir angle	-0.2	0.64	deg^2	3195	0.61
Significant wave height	0	11	m	3145	0.60
AMR wet tropospheric correction	-0.5	-0.001	m	310	0.06
Altimeter wind speed	0	30	$m.s^{-1}$	6824	1.30
Global statistics of edited measurements by thresholds	_	_	_	19685	3.75

TABLE 1: *Table of parameters used for editing.*

The measurements rejected during the editing process are shown in figure 2. Out of over land data, rejected measurements are mainly situated in ice regions and in regions with disturbed sea state.

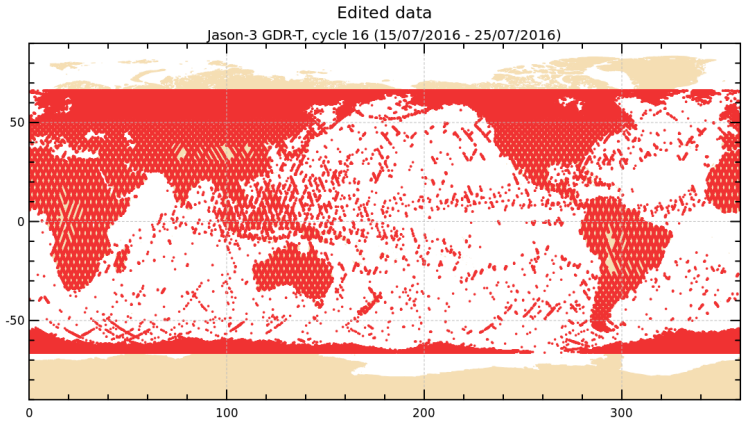

FIGURE 2 – *Edited measurements for cycle 016.*

Map in figure 3 shows the percentage of valid measurements by sample over oceans and seas. Wet zones or zones with sea ice appear in the plot as regions with less valid data, as it was also the case for Topex, Poseidon-1, Jason-1 and Jason-2 altimeters : measurements may be corrupted by rain or sea ice. They were therefore removed by editing. As for Jason-2 there are less removed data in these zones and in the areas of strong sea states compared with the usual maps obtained for Topex or Jason-1.

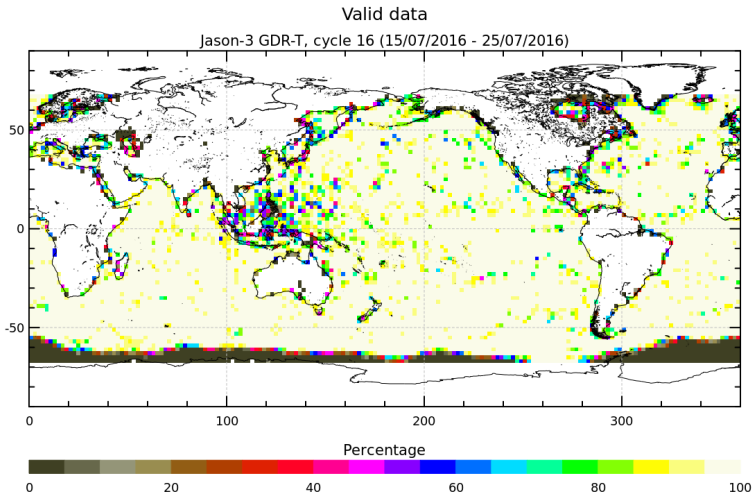

FIGURE 3 – *Percentage of valid measurements for cycle 016.*

3. Instrumental and geophysical parameter analysis

Monitoring of instrumental and geophysical parameters is important in order to detect possible problems. When monitoring parameters over long periods, possible drifts or jumps can be detected. These verification products are produced operationally so that they allow systematic monitoring of the main relevant parameters. When possible, comparison with Jason-2 data are done.

3.1. Jason-3 altimeter and sensor

This section presents the general status of the altimeter for main instrumental variations through the Jason-3 mission. Two calibration modes are used to monitor the altimeter internal drifts and compute the altimetric parameters. They are programmed about three times per day, over land.
The CAL1 mode measures the Point Target Response (PTR) of the altimeter in Ku and C bands. Among the parameters extracted from the PTR are :

— the internal path delay
— the total power of the PTR

The evolutions of these parameters as a function of time are plotted to monitor the ageing of the altimeter.
The CAL2 mode measures the low pass filter of the altimeter in Ku and C bands.

Notice that in the Jason-3 products, the range is corrected for the internal path delay and the backscatter coefficient takes into account the total power of the measured PTR.

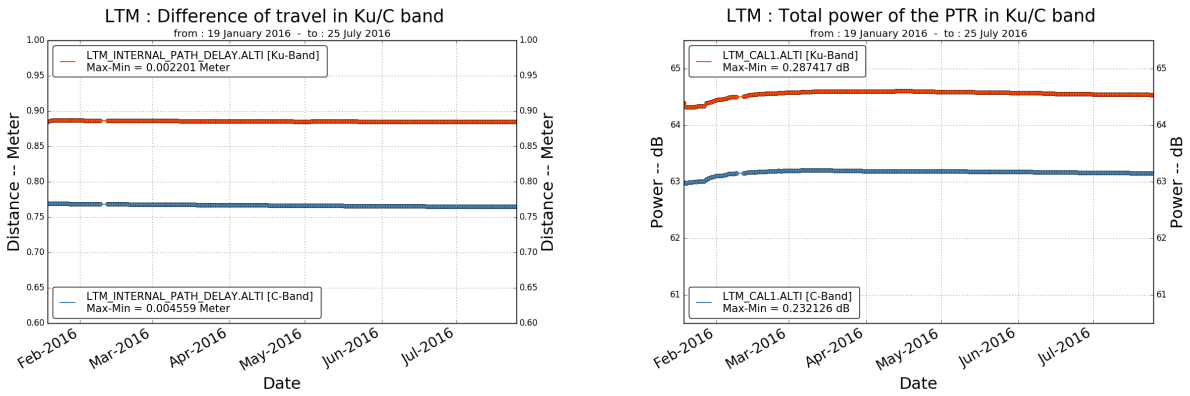

FIGURE 4 – *Internal path delay (left) and total power of the PTR (right) for Ku- and C-band.*

3.2. Significant wave height

Figure 5 shows wave estimations derived from altimeter measurements. Therefore significant wave height data from the current cycle are averaged over a grid of 2° by 2° resolution . Wave height may reach several meters.

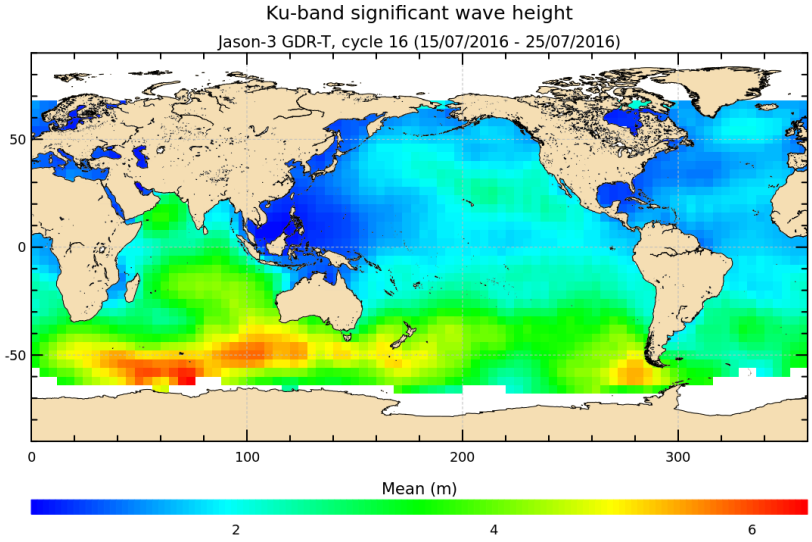

FIGURE 5 – *Significant wave height for cycle 016.*

The daily average of Ku-band SWH for Jason-3 and Jason-2 is plotted as a function of time on figure 6. They show similar features.

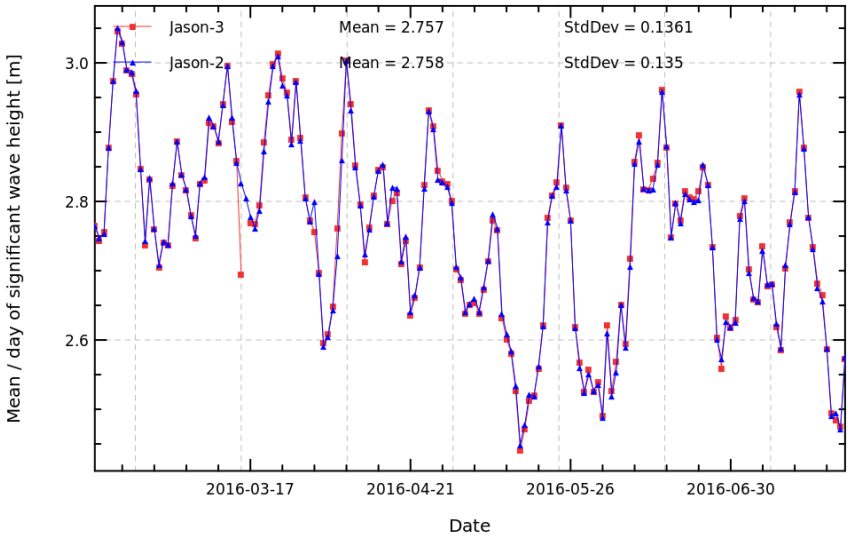

FIGURE 6 – *Daily monitoring of Ku-band significant wave height for Jason-2 and Jason-3.*

3.3. Backscattering coefficient

The daily average of Ku-band backscattering coefficient for Jason-2 and Jason-3 is plotted as a function of time on figure 7. Beside a bias, they show similar features.

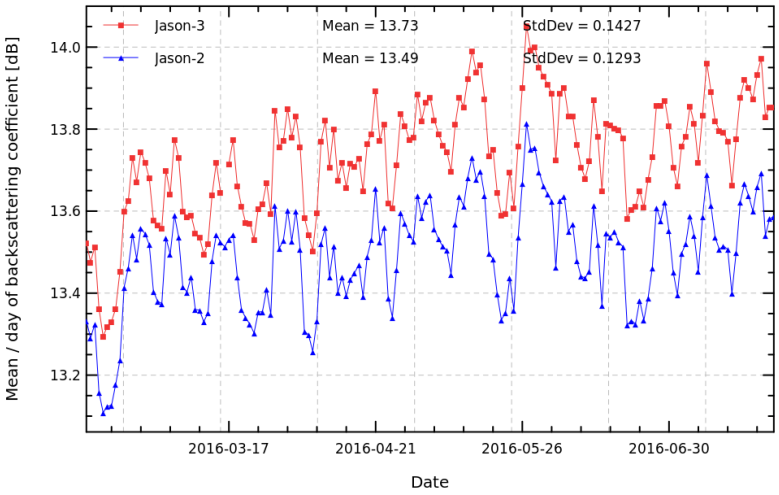

FIGURE 7 – *Daily monitoring of Ku-band backscattering coefficient for Jason-2 and Jason-3.*

3.4. Dual frequency ionosphere correction

The daily average of dual-frequency ionosphere correction for Jason-3 and Jason-2 is plotted as a function of time on figure 8. They show similar features, but a bias is visible. This bias comes from Ku and C-band range differences between Jason-3 and Jason-2.

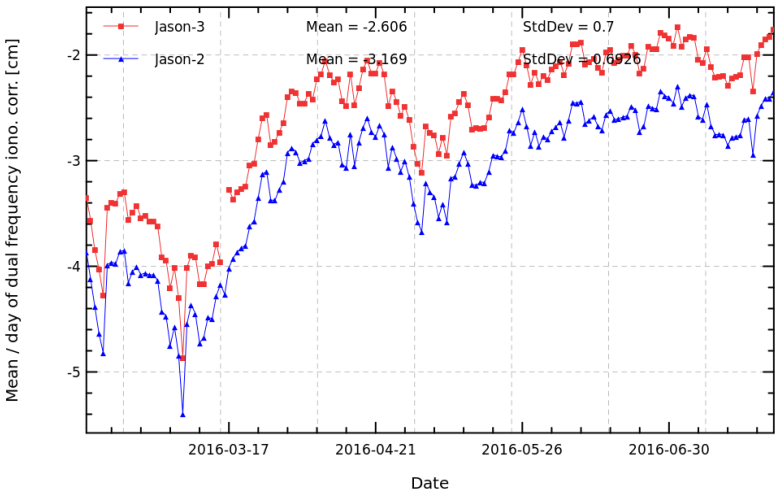

FIGURE 8 – *Daily monitoring of dual-frequency ionosphere correction for Jason-2 and Jason-3.*

3.5. Altimeter wind speed

Figure 9 shows altimeter wind estimations derived from altimeter measurements. Therefore the data from the current cycle are averaged over a grid of 2° by 2° resolution.

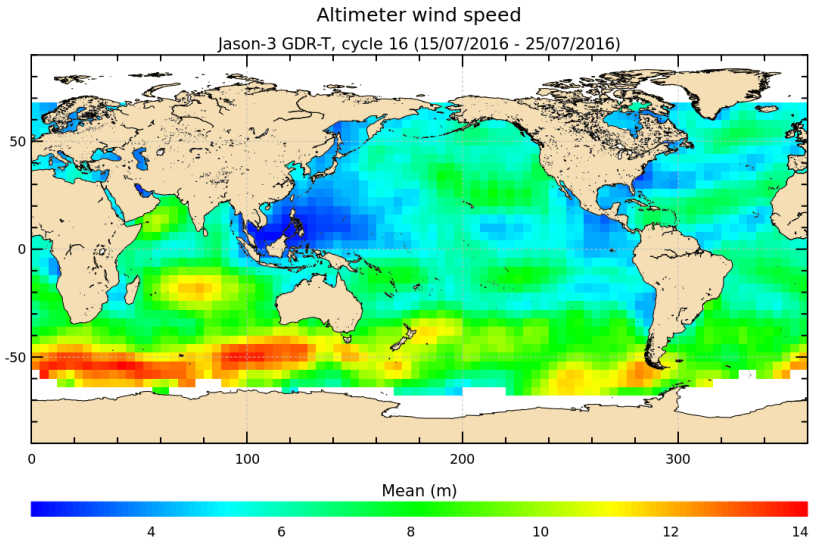

FIGURE 9 – *Altimeter wind speed for cycle 016.*

The daily average of altimeter wind speed for Jason-3 and Jason-2 is plotted as a function of time on figure 10. Since 16-03-2016 (platform pointing change, impacting sigma0 and so wind speed), a small bias has been visible between Jason-2 and Jason-3. Except this bias, they show similar features.

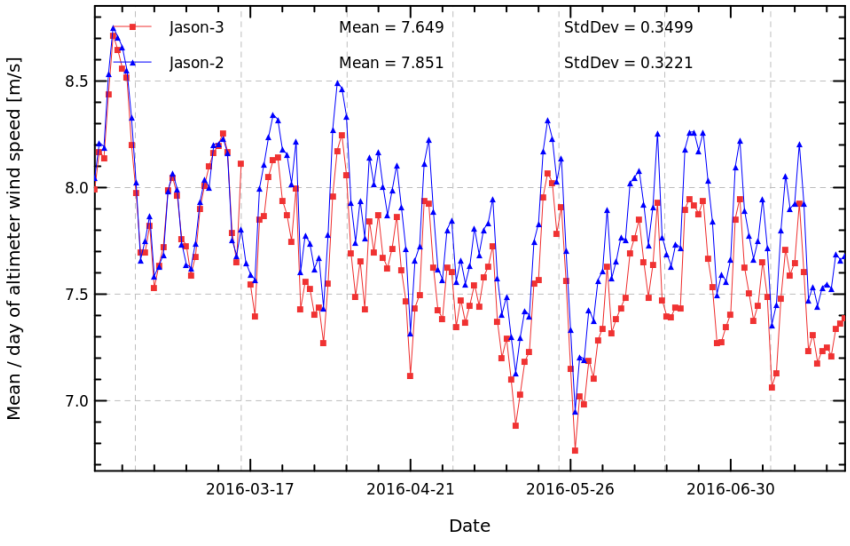

FIGURE 10 – *Daily monitoring of altimeter wind speed for Jason-2 and Jason-3.*

3.6. Radiometer parameters

The left part of figure 11 shows the mean and standard deviation of wet troposphere correction (radiometer - ECMWF) difference by pass for current cycle. Beside natural pass to pass variations, there is no anomaly detectable.

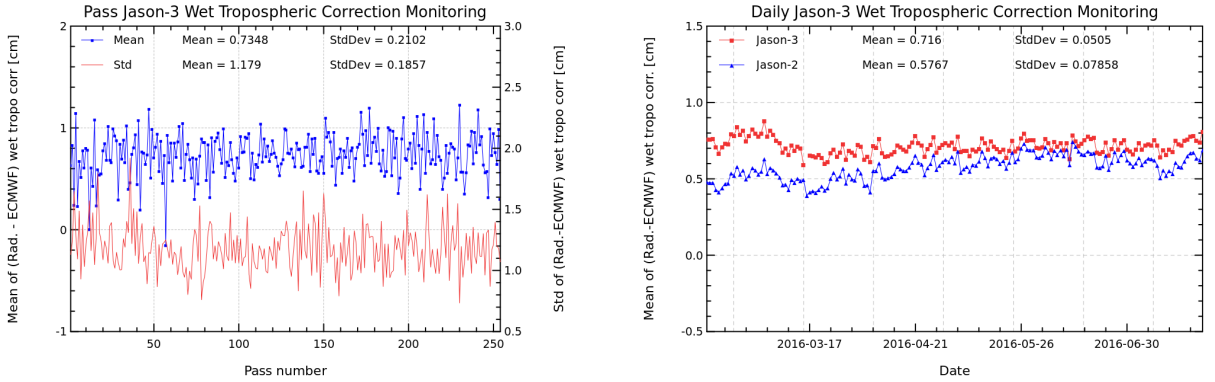

FIGURE 11 – *Pass monitoring of wet troposphere differences between radiometer and ECMWF model for Jason-3 cycle 016 (left) and Jason-3 versus Jason-2 daily monitoring of wet troposphere differences between radiometer and ECMWF model (right).*

For Jason-3 as for Jason-2, an Autonomous Radiometer Calibration System (ARCS) is used prior to GDR production for the Jason-3 radiometer (AMR) in order to monitor calibrations and recalibrate if necessary (for more details see [3] dealing with Jason-2 system). The plot of daily means of (Radiometer - ECMWF) wet troposphere correction was quite stable, even though ARCS does not use the ECMWF model to calibrate the AMR. Nevertheless small variations of up to 2 mm amplitude are observable. They can be due to (among others) evolution of ECMWF model or ARCS calibrations. Though for GDR, these drifts and jumps are approximatively corrected by ARCS (by discrete values), drifts are still visible within a cycle. Furthermore, the application of a discrete recalibration can also lead to jumps in the time series. Note that Jason-3 AMR have been recalibrated about every 2 months with cold sky calibration.

4. Crossover Analysis

4.1. Overview

SSH crossover differences are the SSH differences between ascending and descending passes where they cross each other. Crossover differences are systematically analyzed to estimate data quality and the Sea Surface Height (SSH) performances. SSH crossover differences are computed from the valid data set on a one cycle basis, with a maximum time lag of 10 days, in order to limit the effects of ocean variability which are a source of error in the performance estimation. The mean SSH crossover differences should ideally be close to zero and standard deviation should ideally be small.

Nevertheless SLA varies also within 10 days, especially in high variablity areas. Furthermore, due to lower data availability (due to seasonal sea ice coverage), models of several geophysical corrections are less precise in high latitude. Therefore an additional geographical selection - removing shallow waters, areas of high ocean variability and high latitudes ($> |50|$ deg) - is applied for cyclic monitoring.

4.2. Maps of SSH crossover differences

After data editing, applying additional geographical selection and using the standard Jason-3 algorithms, the crossover standard deviation is about 5.16 cm rms.
The map of the mean differences at crossovers (4 by 4 degrees by bins) is plotted for the current cycle on left panel of figure 12, whereas the right panel shows the whole Jason-3 period.

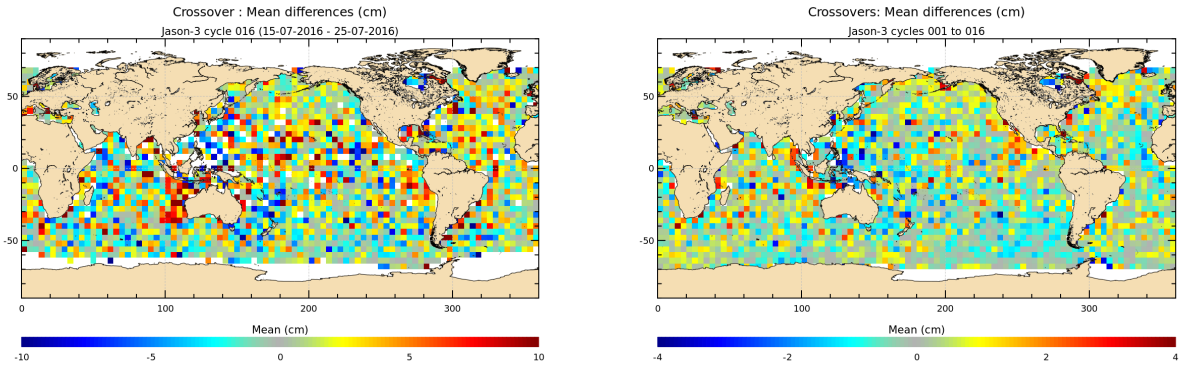

FIGURE 12 – *Mean SSH at crossovers for cycle 016 (left) and over the whole Jason-3 period (right).*

4.3. Cycle by cycle monitoring

The mean and standard deviation of SSH differences at crossovers are plotted for Jason-3 and Jason-2 as a function of time on a one cycle per cycle basis in figure 13. Note that cycle 001 of Jason-3 corresponds to cycle 281 of Jason-2. The statistics are computed after data editing and using the geographical selection criteria.

A signal seems to appear on Jason-3 SSH differences at crossover (this is under investigation).

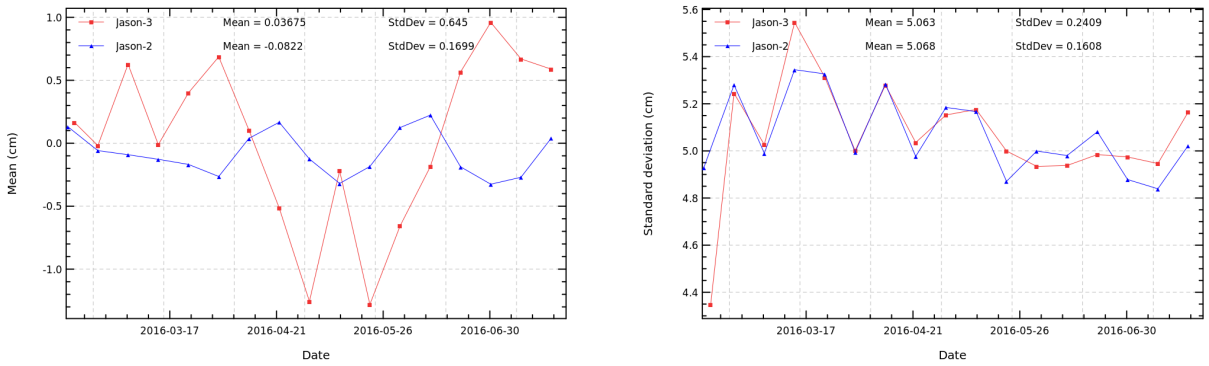

FIGURE 13 – *Cyclic monitoring of mean (left) and standard deviation (right) of SSH differences at crossovers for Jason-3 and Jason-2.*

Figure 14 shows the mean and the standard deviation of Jason-2 − Jason-3 10-day SSH crossovers, using radiometer wet troposphere correction for both satellites or ECMWF model wet troposphere correction.

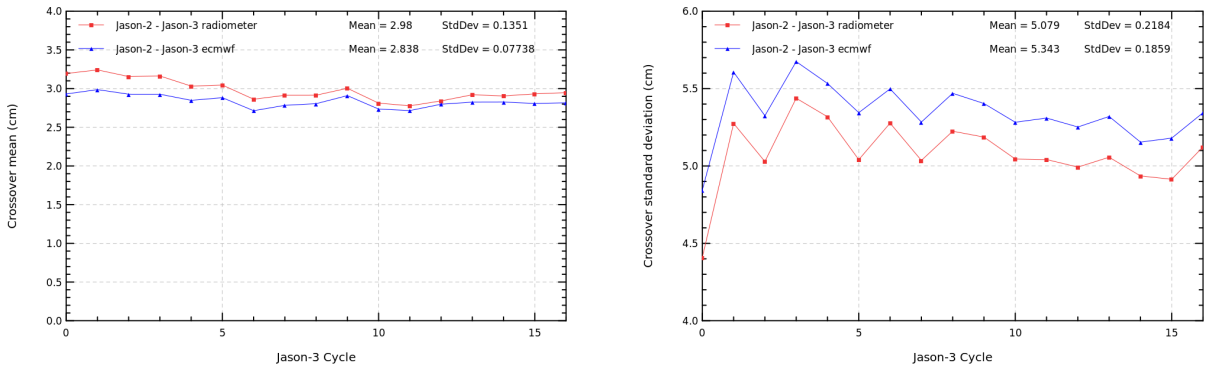

FIGURE 14 – *Cyclic monitoring of mean (left) and standard deviation (right) of (Jason-2 − Jason-3) SSH differences at crossovers.*

4.4. Comparison of pseudo time tag bias

The pseudo time tag bias is found by computing at SSH crossovers a regression between SSH and orbital altitude rate ($\dot{H}$), also called satellite radial speed :

$$SSH = \alpha \dot{H}$$

This method allows us to estimate the time tag bias but it absorbs also other errors correlated with $\dot{H}$ as for instance orbit errors. Therefore it is called "pseudo" time tag bias.

The monitoring of this coefficient estimated at each cycle is performed for Jason-3 and Jason-2 in the following figure : it hightlights that pseudo time tag bias is close to zero (mean value) for both missions.

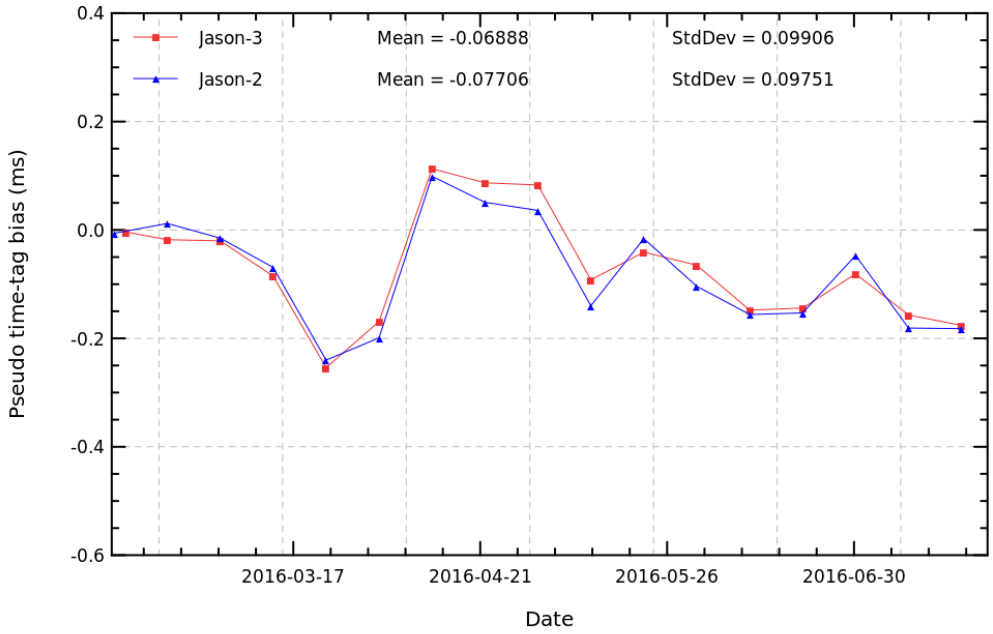

FIGURE 15 – *Cyclic monitoring of pseudo time tag bias for Jason-3 and Jason-2.*

5. Along track analysis

5.1. Mean of along-track SLA

5.1.1. Temporal analysis

The monitoring of mean SLA for Jason-3 and Jason-2 (Figure 16 on left) and the monitoring of mean SLA differences between both missions (Figure 16 on right) show a very stable bias (close to 3.0 cm).

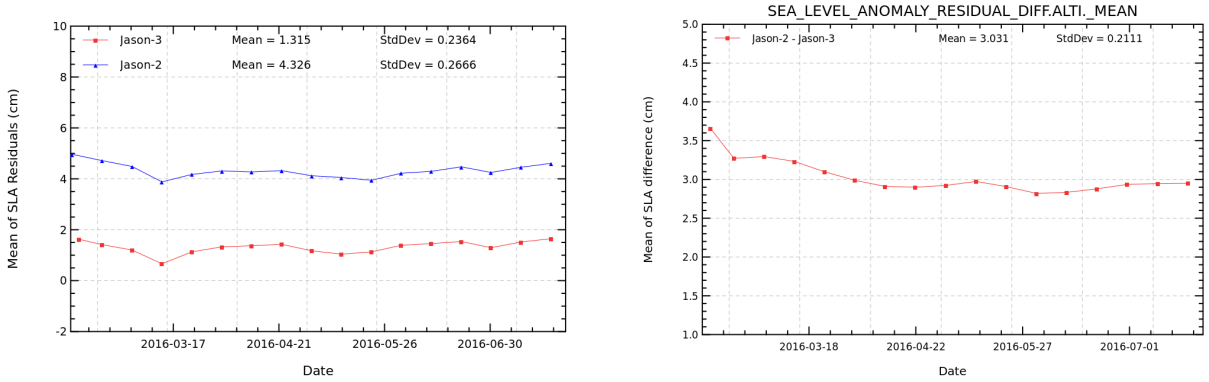

FIGURE 16 – *Cyclic monitoring of mean SLA for Jason-3 and Jason-2 (left) and differences of (Jason-3 – Jason-2) mean SLA (right).*

5.1.2. Maps

Figure 17 show the map of Jason-3 SLA relative to the MSS.

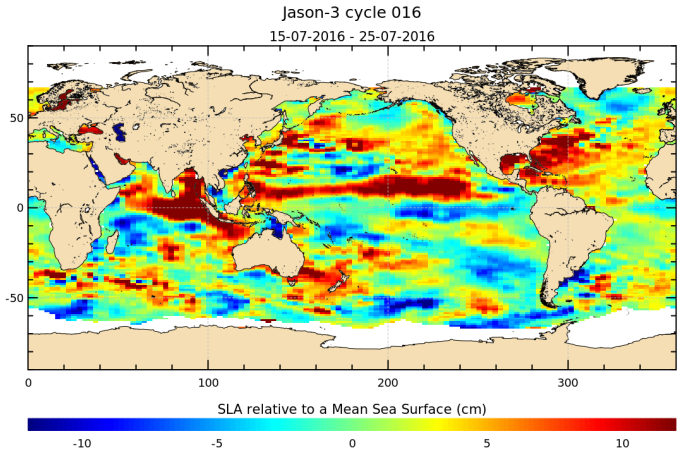

FIGURE 17 – *Sea level anomaly relative to MSS for cycle 016.*

As during the tandem phase (cycle 001 to 023) both satellites measure the same oceanic features only 1’20" apart, direct SLA differences (without applying corrections) are possible. They are shown for the current cycle on figure 18. There are only weak geographical biases visible (likely due to differences in orbit processing).

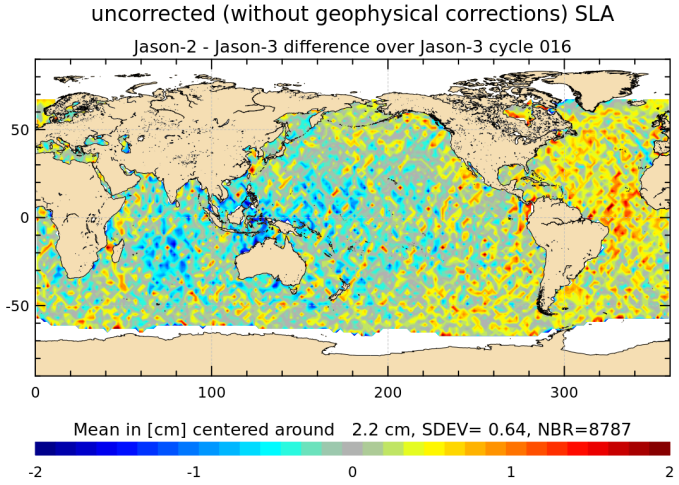

FIGURE 18 – *Jason-2 − Jason-3 SLA differences (without corrections) for cycle 016.*

5.2. Along-track performances

Sea Level Anomaly (SLA) statistics are computed from repeat-track analysis. The plot below gives the standard deviation of the SLA for each cycle over the whole data set.

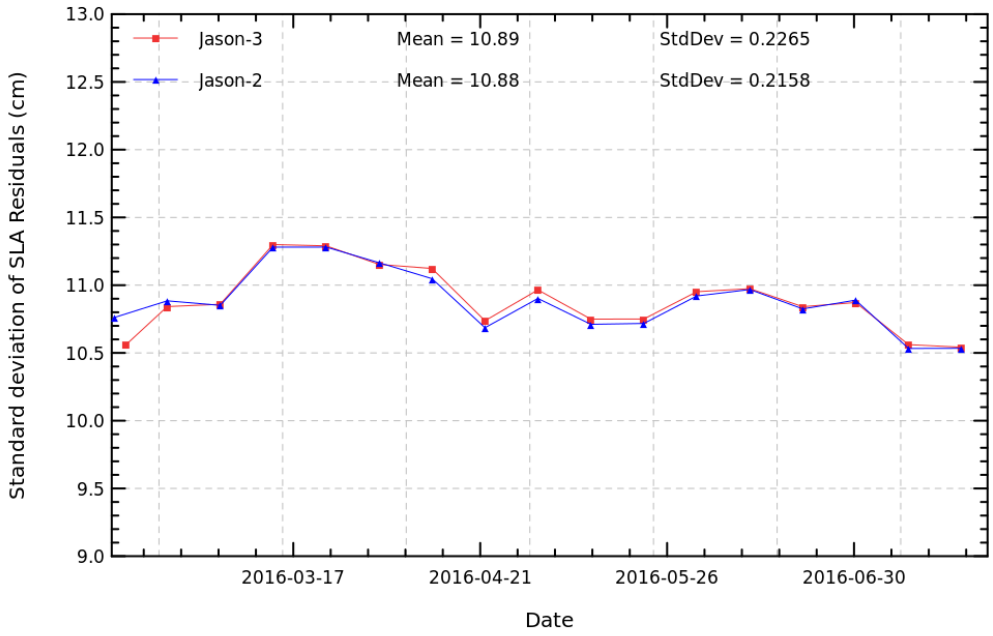

FIGURE 19 – *Cyclic monitoring standard deviation of along track SLA for Jason-3 and Jason-2.*

Références

[1] Jason-3 Products Handbook, February 2016 *SALP-MU-M-OP-16118-CN*. Available at : www.aviso.altimetry.fr/fileadmin/documents/data/tools/hdbk_j3.pdf

[2] M. Ablain, Cazenave, A., Valladeau, G., and Guinehut, S. 2009 : A new assessment of the error budget of global mean sea level rate estimated by satellite altimetry over 1993-2008. *Ocean Sci,* **5,** 193-201. Available at http://www.ocean-sci.net/5/193/2009/os-5-193-2009.pdf *Ocean Sci,* **5,** 193-201. Available at http://www.ocean-sci.net/5/193/2009/os-5-193-2009.pdf

[3] S. Brown, S. Desai, W. Lu, and A. Sibthorpe. 2009 : Performance assessment of the Advanced Microwave radiometer after 1 year in Orbit. *OSTST Seattle, USA,*. Available at : www.aviso.altimetry.fr/fileadmin/documents/OSTST/2009/oral/Brown.pdf

[4] J.-D. Desjonqueres, G. Carayon, J.-L. Courriere, and N. Steunou, 2008. Poseidon 3 In-flight results. *OSTST Nice, France*. Available at : www.aviso.altimetry.fr/fileadmin/documents/OSTST/2008/oral/desjonqueres.pdf